Perifornical Area Urocortin-3 Neurons Promote Infant-directed Neglect and Aggression

Anita E Autry[1,2], Zheng Wu[1,3], Johannes Kohl[1,4], Dhananjay Bambah-Mukku[1], Nimrod D

Rubinstein[1,5], Brenda Marin-Rodriguez[1], Ilaria Carta[2], Victoria Sedwick[2], & Catherine Dulac[1]

[1] Howard Hughes Medical Institute, Department of Molecular and Cellular Biology, Center for

Brain Science, Harvard University, Cambridge, Massachusetts 02138, USA.

[2] Dominick P. Purpura Department of Neuroscience, Department of Psychiatry and Behavioral

Sciences, Albert Einstein College of Medicine, Bronx, NY 10461, USA.

[3] Current Address: Mortimer B. Zuckerman Mind Brain Behavior Institute and Department of

Neuroscience, Columbia University, New York, NY 10027, USA.

[4] Current Address: The Francis Crick Institute, London, UK.

[5] Current Address: Calico Life Sciences, LLC, 1170 Veterans Blvd, South San Francisco, 94080,

USA

.

1

SUMMARY

Mammals invest considerable resources in protecting and nurturing young offspring. However, under certain physiological and environmental conditions, animals neglect or attack young conspecifics. Males in some species attack unfamiliar infants to gain reproductive advantage[1-3] and females kill or neglect their young during stressful circumstances such as food shortage or threat of predation[4-8]. In humans, stress is a risk factor in both sexes for peripartum disorders and associated impairments in parent-infant interactions[9]. While recent studies have uncovered dedicated neural pathways mediating the positive control of parenting[10-13], the regulation of infant-directed neglect and aggression and the relationship between these behaviours and stress are poorly understood. Here we show that urocortin-3 (*Ucn3*)-expressing neurons in the perifornical area (PeFA^Ucn3) of the hypothalamus are activated during infant-directed attacks in males and females, but not other forms of aggression. Opto- and chemogenetic manipulations of PeFA^Ucn3 neurons demonstrate the role of this neuronal population in the negative control of parenting in both males and females. PeFA^Ucn3 neurons receive input from areas associated with vomeronasal sensing, stress, and parenting, and send major projections to the ventromedial hypothalamus (VMH), ventral lateral septum (LSv) and amygdalohippocampal area (AHi). Optogenetic activation of PeFA^Ucn3 axon terminals in these regions triggers different aspects of infant-directed agonistic responses, such as neglect and aggression. Thus, PeFA^Ucn3 neurons emerge as a critical hub for the expression of infant-directed neglect and aggression, providing a new framework to examine the positive and negative regulation of parenting.

RESULTS

Urocortin-3 expressing cells in the perifornical area are specifically activated during infant-directed aggression

To identify brain areas involved in infant-directed aggression, we monitored the induction of the immediate early gene (IEG) *c-fos* across the hypothalamus and septal and amygdaloid nuclei in

2

infanticidal virgin males, fathers, and mothers after interactions with pups (Fig. 1a-b). Significantly more *c-fos* positive cells were found in the medial bed nucleus of stria terminalis (BNSTm), the LSv, and PeFA of infanticidal males compared to mothers and fathers, with the most robust differences observed in the PeFA, a small nucleus between the fornix and the paraventricular hypothalamus (PVH) (Fig. 1a, b). By contrast, fewer *c-fos* positive cells were observed in the medial preoptic area (MPOA) of infanticidal males compared to mothers, as expected from previous studies[13,14] (Fig. 1a, b). To identify markers of PeFA cells activated by infant-directed attacks, we visualized *c-fos* expression in tissue sections from virgin males after interactions with pups and performed microdissections of the corresponding areas in adjacent sections followed by gene expression analysis of the micro-dissected material (Fig. 1c). Expression analysis (see Methods) revealed 267 genes with significant differential expression between the *c-fos* positive area and the adjacent hypothalamic tissue, with two genes, vasopressin (*Avp*) and *Ucn3*, showing the largest differences (Fig. 1d; $p < 0.002$ and $p < 0.003$ respectively). Phosphorylated-S6 ribosomal pulldown[15] after pup-directed attack further confirmed *Ucn3* as enriched in neurons activated by infanticide (Supp. Fig. 1a). *Ucn3* expression appeared spatially restricted to the PeFA (Fig. 1e) with the highest colocalization with *c-fos*+ cells after infanticide (55.3% cfos+ cells co-express *Ucn3*) compared to AVP (7.5% cfos+ cells co-express AVP) (Supp. Fig. 1b). Notably, while *Ucn3*+ cells were found throughout the PeFA, *Ucn3*+/*c-fos*+ neurons identified after infant-directed attack were located primarily in the rostral half of the PeFA (Fig. 1f).

Next, we asked whether the activity of *Ucn3*-positive PeFA neurons (PeFA^{Ucn3}) neurons was specifically associated with infant-directed agonistic interactions or generally increased by aggressive displays. Remarkably, *c-fos* expression was induced in PeFA^{Ucn3} neurons after pup-directed attacks by virgin males and females, but not after any other forms of aggression such as maternal defense, inter-male aggression, or predation, nor by stress or feeding behaviour, suggesting a specific role of this population in infant-directed aggression in both sexes (Fig. 1h).

3

Few PeFA[Ucn3] neurons were activated in virgin females engaged in pup retrieval to the nest, while this population was entirely silent in lactating females (Fig. 1h). No difference was observed in the number of PeFA[Ucn3] neurons in virgin versus mated males or females (Supp. Fig. 1c). Most PeFA[Ucn3] neurons expressed the vesicular glutamate transporter 2 (vglut2) suggesting an excitatory function (Supp. Fig. 1d). Thus, *Ucn3*-positive neurons of the rostral PeFA are specifically activated by pup-directed aggression, but no other forms of adult aggression or other behaviours.

Inhibition of PeFA[Ucn3] neuronal activity in virgin males blocks infanticide

To test if PeFA[Ucn3] neuronal activity is required for the display of male infanticide, we used a conditional viral strategy to express the inhibitory opsin NpHR3.0, or yellow fluorescent protein (YFP) as a control, in PeFA[Ucn3] neurons and implanted bilateral optical fibres above the PeFA of virgin males (Fig. 2a, Supp. Fig. 2a). Before laser stimulation, control and NpHR3.0-injected males showed similarly high levels of pup-directed aggression with short latencies to attack (Fig. 2b-d). By contrast, optogenetic inhibition of PeFA[Ucn3] neurons led to a reduction in the number of males displaying pup-directed attacks, an increase in attack latency, and a decrease in the duration of aggressive displays toward pups (Fig. 2 b-d). Strikingly, the suppression of pup-directed aggression persisted – and even further increased – within the next 24h, suggesting a long-term effect of acute PeFA[Ucn3] neuronal silencing (Fig. 2b-d, 2nd 'laser-off' session). Males spent equivalent time investigating pups in all conditions and did not increase their parental behaviours within the test period (Fig. 2e, f). Likewise, PeFA[Ucn3] silencing did not affect motor activity or adult intruder-directed aggression (Fig. 2g). These data suggest that PeFA[Ucn3] neuron activity is required for the regulation of pup-directed aggression.

Activation of PeFA[Ucn3] neurons elicit infant-directed neglect in virgin females

4

To test if the activity of PeFA[Ucn3] neurons was sufficient to trigger infant-directed agonistic interactions in females, we used conditional viruses to express the excitatory opsin Channelrhodopsin-2 (ChR2), or YFP control, in PeFA[Ucn3] neurons (Fig. 2h, Supp. Fig. 2b). Parenting experience strongly impacts subsequent interactions of virgin females with pups[16] and indeed, sessions in which the laser off condition was tested first led to irreversible parental behaviour in mice injected with ChR2 (Supp. Fig. 2c, d). Hence, all sessions were started with the laser ON condition in both experimental and control groups, followed by laser OFF in the second session, and back to laser ON in third session (see methods). As expected, control females became increasingly more parental from session to session, with more pups retrieved and with shorter latencies in each subsequent session (Fig. 2i, j, left panels). By contrast, optogenetic stimulation of PeFA[Ucn3] neurons reduced female parenting with fewer pups collected and with longer latencies in the third session compared to first (laser ON) and second (laser OFF) sessions (Fig. 2i, j right panels). Further, the duration of parental behaviours, investigation bout length, and time spent in the nest with pups were significantly reduced in the third compared to earlier sessions, and parental behaviour and time spent in the nest with pups was significantly reduced between control and ChR2 females in the third trial (Fig. 2 k, l), and fewer females in the ChR2 group retrieved pups to the nest (Fig 2m). While the overall display of pup-directed aggression (duration of aggression and number of females displaying aggression) was not significantly increased (Fig. 2n), a subset of females (n = 3 /15) showed tail-rattling locked to laser stimulation, an overt sign of aggression never observed in control females (Supp. Video 1). Further, activation of PeFA[Ucn3] neurons did not affect motor activity or intruder-directed aggression (Fig. 2o). Consumption of appetitive food was slightly decreased with activation of PeFA[Ucn3] neurons in ChR2 females (Supp. Fig. 2e), in agreement with the previously reported anorexigenic effect of this neural population[17,18].

To confirm the effects of PeFA[Ucn3] neuron activation and assess the effects of prolonged activation in virgin females, we injected a conditional virus expressing the excitatory chemogenetic effector

5

hM3Dq followed by administration of its ligand clozapine-*n*-oxide (CNO) (Fig. 2p, Supp. Fig. 2f). Chemogenetic activation of PeFA[Ucn3] neurons led to a decrease in pup retrieval compared to control (Cre negative) females (18% pups retrieved versus 70%, Fisher's exact test p<0.0015) (Fig. 2q; Kolmogorov-Smirnoff test p<0.001). Further, fewer experimental females displayed parental behaviours compared to controls, and we observed a decrease in overall parental behaviour, reduced time in the nest with pups, and reduced nest building (Fig. 2r, s). Pup-directed aggression was observed in some females after activation of PeFA[Ucn3] neurons, and despite diminished parenting, females with activated PeFA[Ucn3] neurons investigated pups as much as control females, suggesting they were not avoidant (Fig. 2t). Together, these data suggest that activation of PeFA[Ucn3] neurons reduced parenting in virgin females, and induced signs of aggression in a subset of females.

PeFA[Ucn3] neurons receive input from parenting and stress-associated cell populations

To identify monosynaptic inputs to PeFA[Ucn3] neurons, we used conditional rabies virus mediated retrograde trans-synaptic tracing in adult virgin males and females[19] (Fig. 3a). Fifteen brain areas were found to provide monosynaptic inputs, all located exclusively within the hypothalamus, lateral septum, and medial amygdala, with the highest fraction of inputs originating from PVH, MPOA, and anterior hypothalamus (AH) (Fig. 3b-d). The PVH contained the highest fractional inputs to PeFA[Ucn3] neurons in both sexes, with a higher fraction in females (44.92% ± 8.1%) as compared to males (22.95% ± 4.2%) (Fig. 3d). PVH inputs were comprised of AVP (31.9% ± 11.1%), CRH (17.8% ± 7.1%) and OXT (9.1% ± 2.1%) expressing cells, i.e. populations implicated in social and stress responses[20-23], while around half (48.02%) of PeFA[Ucn3] monosynaptic inputs from the MPOA originated from galanin-positive cells, a largely GABAergic neural population involved in the positive control of parenting[11,13] (Figure 3e, f). Thus, PeFA[Ucn3] neurons are poised to receive major inputs from vomeronasal and hypothalamic pathways associated with stress, social information, and parenting.

6

These data prompted us to test the effect of stress on pup interactions and PeFA^{Ucn3} neuronal activity. Confirming previous reports[24,25], chronic restraint stress in virgin females led to weight loss, reduced pup retrieval, and a decreased fraction of parental females (Fig. 3g-i). No difference was observed in the number of *c-fos* positive PeFA^{Ucn3} neurons in stressed females interacting with pups as compared to unstressed controls females. However, strikingly, while an inverse correlation was observed between PeFA^{Ucn3} neuronal activation and parental behaviour in control females ($R^2 = 0.52$), chronic restraint stress entirely abolished this relationship ($R^2 = 0.14$) (Fig. 3k; slope difference p<0.0055). Together these data show that PeFA^{Ucn3} neurons function as a critical node between vomeronasal, stress, and parenting-related neural pathways, and suggest that chronic stress disrupts their normal function.

PeFA^{Ucn3} neurons project to areas involved in aggression and anxiety

Next, we visualized PeFA^{Ucn3} axons and presynaptic terminals by conditional viral expression of tdTomato and synaptophysin-eGFP (Fig. 3l). All observed PeFA^{Ucn3} projections were within hypothalamus, lateral septum, median eminence, and amygdalo-hippocampal area (AHi), with the most densely labelled projections in AHi, LSv, PVH, and VMH (Fig. 3m-o). No obvious sex differences were observed (Fig. 3m-o).

To understand the functional organization of PeFA^{Ucn3} neuronal projections, we performed pairwise injections of fluorophore conjugated cholera toxin B subunit (CTB-488 and CTB-647) retrograde tracers (Fig 3p, q). We focused on PeFA^{Ucn3} projections to LS, AHi, and VMH, based on their dense labelling (Fig. 3m-o) and the known functions of these target areas in stress and aggression[26-33]. For each paired target injection, around 50-60% of PeFA^{Ucn3} neurons were labelled by both tracers (Fig. 3r), suggesting that individual PeFA^{Ucn3} neurons project to multiple targets. To further determine the involvement of these projection areas in pup-directed aggression, we performed CTB-mediated retrograde tracing from LS, VMH, and AHi individually and quantified the overlap between CTB labelling and C-Fos expression in the PeFA of virgin

7

males after pup interactions (Fig. 3s, t). C-Fos labeling was found in each of the three major projections, with AHi-projecting C-Fos+ cells preferentially located in the rostral and medial subdivision of PeFA (Fig. 3u; Supp. Fig. 3a). Together, these results suggest that PeFA[Ucn3] neurons send out branched projections, and that all major projections are equivalently active during pup-directed attacks with preferential involvement of rostro-medial PeFA projections to AHi.

PeFA[Ucn3] neuronal projections govern discrete aspects of infant-directed neglect and aggression

To test the respective functions of PeFA[Ucn3] projections, we performed optogenetic activation of PeFA[Ucn3] terminals in virgin females injected in the PeFA with a conditional ChR2-expressing virus and with optical fibres implanted bilaterally above each projection target. We initially focused on projections to VMH, based on the documented role of this area in the control of aggression[30,32] (Fig 4a). Stimulation of PeFA[Ucn3] to VMH projections reduced pup retrieval across sessions and shortened individual bouts of pup investigation (Fig. 4b; Supp. Video 2). However, it did not affect the overall number of parental females nor the overall time engaged in parental interactions, latency to retrieve, time spent in the nest with pups, and pup grooming (Fig. 4c-e). Further, we did not observe any pup-directed aggression (Fig. 4f). Thus, activating PeFA[Ucn3] to VMH projections inhibits sustained interactions with pups and pup retrieval, but does not elicit aggression toward pups.

We next stimulated PeFA[Ucn3] to LS projections (Fig. 4g) and found that this manipulation inhibited parental behaviour in a significant fraction of females, as well as reduced cumulative pup retrieval and pup grooming across the three sessions (Fig. 4 h, i). Moreover, stimulation of PeFA[Ucn3] to LS projections triggered instances of pup-directed aggression (such as aggressive handling and biting) in 30% of females, although the overall time displaying aggression remained negligible (Fig. 4j). PeFA[Ucn3] to LS stimulation had no significant effect on time spent

8

in the nest with pups, pup investigation, overall parenting time, or latency to retrieve (Fig. 4 k, l). In a subset of females (n = 2 / 10), PeFA^{Ucn3} to LS stimulation led to an escape response, which was never observed in other manipulations (Supp. Video 3). Together, these results suggest that PeFA^{Ucn3} to LS projections inhibit parenting and mediate signs of aggression.

Finally, we examined the function of PeFA^{Ucn3} to AHi projections (Fig. 4m) and found that 55% of females displayed infant-directed aggression such as biting and aggressive carrying of pups without completing retrieval in a manner similar to the stereotyped infanticidal behaviours observed in males with increased time displaying aggression (Fig. 4n, Supp. Video 4). Additionally, PeFA^{Ucn3} to AHi stimulation dramatically reduced cumulative retrieval over the course of three sessions, time spent in the nest with pups, number of parental females, and time spent pup-grooming (Figure 4o, p), with no effect on retrieval latency, pup investigation bout length, or time parenting (Fig. 4q, r). Thus, PeFA^{Ucn3} to AHi projections strongly affect the expression of infant-directed aggression and the suppression of parental behaviours. Stimulation of PeFA^{Ucn3} projections to VMH, LS, and AHi did not impact locomotion, appetitive feeding, or conspecific aggression (Supp. Fig. 3b-h). Altogether, these data suggest that various aspects of infant-directed neglect and aggression are mediated across PeFA^{Ucn3} projections, with PeFA^{Ucn3} to VMH projections suppressing pup investigation, PeFA^{Ucn3} to LS projections mediating reduced pup handling and low-level aggression, and PeFA^{Ucn3} to AHi projections inducing stereotyped displays of pup-directed aggression (Fig. 4s).

Concluding Remarks

The last few decades have seen considerable progress in the use of experimental model systems to identify the neural basis of parental behaviour[11-14,34]. These studies have uncovered critical sensory cues underlying parent-infant interactions, as well as the neural circuit basis of specific repertoires of nurturing displays in males and females[11-14,34]. By contrast, the neural control of infant-directed aggression remains largely unaddressed. Initially considered a

9

pathological behaviour, pioneering work in langurs and other mammals instead suggested that infanticide is an adaptive behaviour that enables males to gain advantage over rivals and females to adapt reproduction to adverse circumstances[1,2]. Although a number of brain areas have been described as negatively affecting parental behaviour[35-40], the existence of a dedicated control hub for infant-directed agonistic interactions, including infanticide, had not yet been explored.

In the present study, we demonstrate that PeFA[Ucn3] neurons are specifically activated by pup-directed aggression in males and females, but not by feeding, conspecific aggression, or acute stress, and that PeFA[Ucn3] neurons are required for infant-directed aggression in males. While activation of PeFA[Ucn3] neurons did not elicit widespread aggression toward pups in females except tail rattling in a subset of animals, we showed that inducing PeFA[Ucn3] neuron activity strongly reduced maternal behaviour including pup retrieval, time in the nest, and overall parenting time. We identified significant direct inputs to PeFA[Ucn3] neurons from largely inhibitory MPOA[Gal] neurons, shown to be critical for the positive control of parenting[11,13]. Because MPOA[Gal] neurons are active in females exposed to pups, MPOA[Gal]-mediated inhibition may repress PeFA[Ucn3] neurons in females and thus occlude the full expression of pup-directed agonistic behaviour during artificial activation of PeFA[Ucn3] neurons.

Previous studies have shown that electrical stimulation of the PeFA leads to a so-called 'hypothalamic rage response' comprising typical aggressive displays including piloerection, teeth baring, and bite attacks[29,30,33]. Indeed, we observe *c-fos* positive neurons in the PVH and PeFA of males and females displaying conspecific aggression, but these neurons are *Ucn3*-negative, suggesting that distinct PeFA populations mediate aggression toward either adults or infants. In addition, *Ucn3* in the PeFA has been implicated in the regulation of social recognition and stress responsivity[18,41-43]. However, our experiments with targeted inhibition or stimulation of PeFA[Ucn3] neurons specifically affected parental behaviour with no effect on adult social

10

behaviours, indicating that PeFA[Ucn3] neurons may be specifically tuned to social cues from infants and/or juveniles rather than adult conspecifics.

Specific tuning of these neurons to social cues is supported by our finding that input areas to PeFA[Ucn3] neurons include the MPOA, MeA, and PVH, known to be essential for integration of social cues sensed by the vomeronasal system which has been well-established as a crucial pathway for infanticide[13,44]. MPOA[Gal] neurons directly send input to PeFA[Ucn3] neurons, suggesting a direct relationship between this well-established hub for pro-parental behaviour and the putative infant-directed aggression neuron population described here. Input neurons from PVH mostly express AVP and CRF, and AVP-expressing PVH neurons have previously been implicated in male-typical social behaviour[20,21], while CRF-expressing PVH neurons are essential mediators of the physiological stress response[45,46]. Our results show that PeFA[Ucn3] neurons do not respond to acute restraint stress, but given their involvement in pup-directed aggression and the role of stress in poor parenting, we reasoned that chronic stress may activate the PeFA[Ucn3] neurons, resulting in decreased maternal behaviour. We found a strong correlation of PeFA[Ucn3] activation and lower levels of parental behaviour in animals under non-stressed conditions suggesting a strong contribution of PeFA[Ucn3] neuron activity to baseline variability in maternal care. Surprisingly, rather than enhancing this relationship, chronic stress disrupted the effect of PeFA[Ucn3] neuron activity on parenting revealing that PeFA[Ucn3] neurons are sensitive to stress in a manner that decouples their activity, as measured by *c-fos* expression, from strength of parental behaviour. Alternatively, PeFA[Ucn3] neurons may be chronically activated during prolonged stress, rendering differences in *c-fos* expression inaccurate to measure changes in neural activity in this cell population during chronic stress.

Previously identified hypothalamic neuronal populations critical for feeding (Agrp neurons in the arcuate nucleus) and parenting (MPOA[Gal] neurons) have been shown to be organized in distinct pools, each largely projecting to a distinct downstream area[11,47]. In contrast, individual PeFA[Ucn3] neurons predominantly project to multiple targets, in a similar manner as

11

VMH neurons extending collaterals to downstream defensive circuits[48]. Interestingly the three major PeFA[Ucn3] target areas VMH, LS and AHi convey overlapping but distinct aspects of infant-directed neglect and aggression (Fig. 4s). Specifically, PeFA[Ucn3] to AHi projections appear to be directly responsible for triggering pup-directed attacks. The function of the AHi is not well understood, although recent data suggest it may send sexually-dimorphic projections to MPOA[Gal] neurons essential for parenting[11]. LS and VMH projections[49-51] appear to play similar roles in the regulation of agonistic interactions with infants. Based on its role in conspecific aggression[32,52], we hypothesized a role for PeFA[Ucn3] to VMH projections in pup-directed attack. However, we found instead that this projection regulates pup investigation. Activation of the PeFA[Ucn3] to LS projections also resulted in sustained reductions in pup interactions, a finding that is consistent with a recent study showing that LS neurons expressing corticotrophin-releasing factor receptor 2 (CRFR2), the high-affinity receptor for *Ucn3*, may control persistent anxiety behaviour[27]. In addition, PeFA[Ucn3] to LS projection activation led to incidences of pup-directed aggression. We noticed that the AHi-projecting neurons that are active during infanticide were located predominantly in the rostral PeFA, as were the majority of PeFA[Ucn3] neurons associated with infanticide. Together with our functional data showing that activation of this projection leads to more pup-directed aggression compared to other projections, we propose that the pattern of activation within subsets of PeFA[Ucn3] neurons defined by their projection targets correlates with the degree of anti-parental behaviour displayed by the individual, from neglect or avoidance, to genuine pup directed attack (Fig. 4s).

Parental behaviour, and by extension infant-directed aggression, is highly regulated by context and previous social experience. Previous studies have shown that females with repeated exposure to pups will become more parental over time[16] . Our experiments with virgin females also showed a similar strong effect of pup exposure on subsequent infant-directed behaviour (Supp. Fig. 2). We observed that males allowed to interact with pups during suppression of PeFA[Ucn3] neurons displayed long lasting reduced aggression toward pups, and

12

that activation of PeFA[Ucn3] neurons in females induced prolonged reduction in parenting. These results stand in contrast to the effects of stimulating MPOA[Gal] neurons, which confers rapid, reversible facilitation of parental behaviour[11,13]. Together, these data suggest that PeFA[Ucn3] neurons may undergo significant functional plasticity or induce long lasting changes in downstream parental circuitry.

Our functional characterization of the PeFA[Ucn3] neurons and their major projection targets uncover this neural population as essential for pup-directed aggression, with specific projections controlling aspects of anti-parental behaviour such as pup investigation and handling as well as stereotyped displays of pup-directed agonistic behaviour. The discovery of a dedicated circuit for pup-directed aggression reinforces the notion that this behaviour might have adaptive advantages in the wild. This study reveals a novel framework for understanding how parental behaviour is modulated at a circuit level and opens new avenues for studying the context- and physiological-state dependent expression of parenting.

Data and code availability statement

The data and code that support the findings of this study are available upon request from the corresponding author.

Ethical statement

All animal experiments were approved by the Harvard University Institutional Animal Care and Use Committee. All experiments were performed in compliance with our Harvard University IACUC approved protocols.

13

Author Contributions

A.E.A. and C.D. conceived and designed the study. A.E.A. performed and analyzed laser capture and microarray, in situ hybridization experiments, pS6 pulldown, optogenetic, chemogenetic, and tracing experiments. Z. Wu helped with study design, laser capture strategy, in situ hybridization experiments, and technical details of optogenetic experiments. J.K. helped with optogenetic experiments, D.B. with pS6 pulldowns, N.D.R. with statistical analysis, B.M.R. with data collection and quantification, I.C. and V.S. with behaviour quantification. A.E.A, Z. W., J.K., D.J.B.M., N.D.R., and C.D. analyzed and interpreted results. A.E.A. and C.D. wrote the manuscript with input from all authors.

Competing Interests

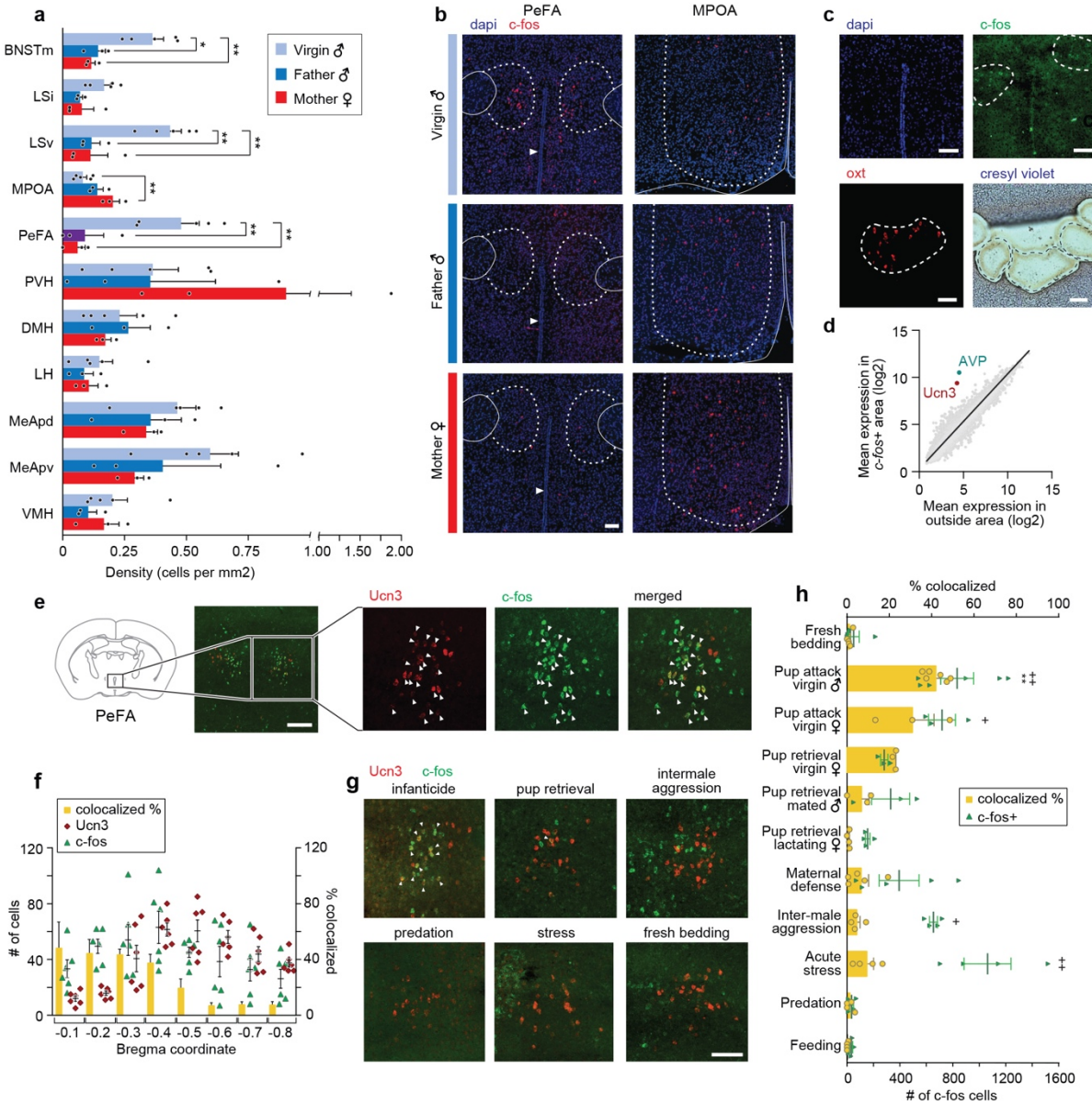The authors declare no competing financial interests.

14

FIGURES

Figure 1. The neuropeptide urocortin-3 (*Ucn3*) in the perifornical area (PeFA) labels neurons activated by infanticide.

a. Quantification of *c-fos* positive cells per mm^2 brain areas of interest in virgin males (attacking), mated males (parental), and mated females (parental) after pup exposure. One-way ANOVA followed by Tukey's multiple comparison test reveals significant differences in medial bed nucleus of stria terminalis (BNSTm) ($F_{2,8}=12.47$, p<0.0035), ventral lateral septum (LSv) ($F_{2,8}=14.31$, p<0.0023), medial preoptic area (MPOA) ($F_{2,8}=8.536$, p<0.0104), and perifornical area (PeFA) ($F_{2,8}=12.02$, p<0.0039) (virgin male n=5; fathers n=3;

15

mothers n=3). b. Representative *in situ* hybridization images of *c-fos* (red channel) expression in PeFA and MPOA after animal exposure to pups with counterstain DAPI (blue channel) (scale bar: 100μm). c. Laser capture strategy to identify markers of cells activated during infanticide (scale bar 100μm). d. Scatter plot displaying relative expression of genes in the *c-fos* positive versus neighboring *c-fos* negative region of the hypothalamus of infanticidal males (n=3 biological replicates, each containing pooled tissue from 6 males; *Avp* p<0.002, *Ucn3* p<0.003). e. Representative in situ hybridization showing colocalization between marker *Ucn3* (red) and *c-fos* induced by infanticide (green) (scale bar 100 μm). f. Number of neurons expressing *c-fos* (green triangles), *Ucn3* (red circles) and both *c-fos* and *Ucn3* (yellow bars) across bregma coordinates (n=6). g. Representative in situ hybridization showing colocalization between expression of *Ucn3* (red) and *c-fos* (green) induced by infanticide and other behaviours (scale bar 100 μm). h. Percentage of *Ucn3*+ cells colocalized with *c-fos* after various behaviours (yellow bars) and number of *c-fos* cells induced by various behaviours (green circles) in the rostral PeFA (n=3-6/group). Kruskal-Wallis test followed by Dunn's multiple comparisons test reveals significant differences in number of *c-fos* positive cells between fresh bedding control exposure and intermale aggression, pup attack in virgin males and virgin females, and acute stress (p<0.0001); yet only pup attack in virgin males reveals significant colocalization between *Ucn3* and *c-fos* (p<0.0002).
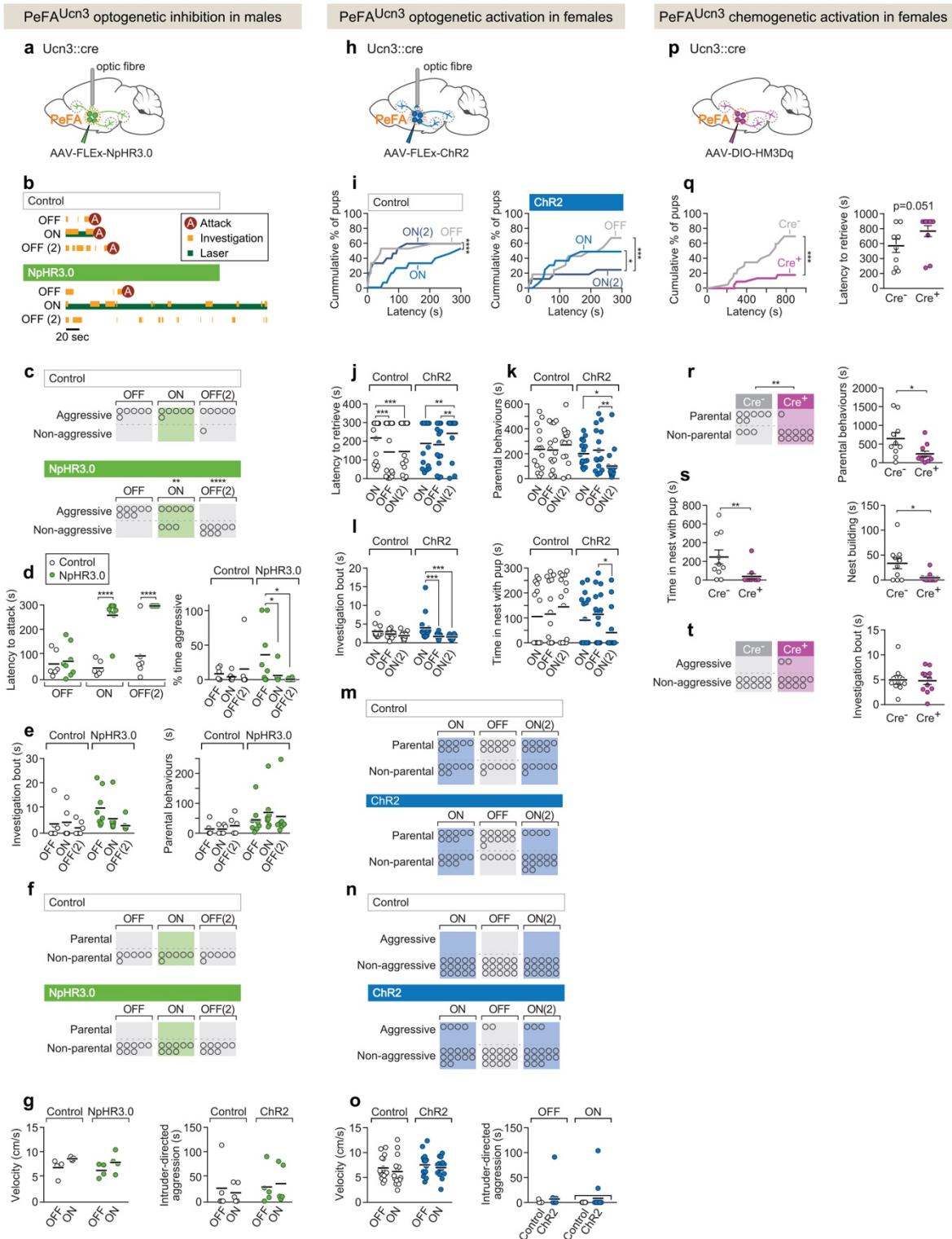
16

Figure 2. PeFA^Ucn3 neurons positively regulate infant-directed aggression at the expense of parental behaviour.

17

a. Setup for optogenetic silencing of PeFA^{Ucn3} neurons in infanticidal virgin males. b. Representative behaviour trace comparing control and halorhodopsin infected males across 3 sessions (scale bar 20 sec of 5 min test). c. Numbers of control and halorhodopsin-expressing males showing aggressive pup-directed behaviour (accelerated failure regression model with first session as time-point baseline and controls as treatment baseline, significant difference between control and halorhodopsin during laser inhibition $p<0.01$ and during second laser off session $p<0.0005$). d. (left) Attack latency across sessions comparing control (open dots; n=6) and halorhodopsin (green dots; n=8) infected males. Two-way repeated measures ANOVA control vs. halorhodopsin $F_{(1,12)}=35.05$, $p<0.0001$, sessions $F_{(2,24)=}22.71$, $p<0.0001$, and interaction $F_{(2,24)}=17.30$, $p<0.0001$ followed by Bonferroni's multiple comparisons test. (right) Percentage of time displaying aggression across 3 sessions in control open dots) and halorhodopsin (green dots) males. Two-way repeated measures ANOVA showed no main effect while post-hoc Tukey's multiple comparisons test revealed significant differences between sessions in the halorhodopsin group. e. (left) Investigation bout length across 3 sessions in control and halorhodopsin males. (right) Duration of parental care behaviours across 3 sessions in control and halorhodopsin males. f. Number of males in control and halorhodopsin-expressing groups displaying parental behaviours. g. (left) Locomotion velocity in control and halorhodopsin-expressing males with and without laser stimulation. (right) Duration of aggression during adult male interactions in control and halorhodopsin-expressing males with and without laser stimulation. h. Setup for optogenetic activation of PeFA^{Ucn3} neurons in virgin female mice. i. (Left) Cumulative retrieval of pups in virgin females injected with a control virus (n=15). Friedman statistic $_{(3, 27)}$ = 41.84 followed by Dunn's multiple comparisons tests. (right) Cumulative retrieval of pups in virgin females injected with ChR2 (n=16). Friedman statistic $_{(3, 24)}$ = 17.19, followed by Dunn's multiple comparisons test. j. Latency to retrieve in control (open dots) and ChR2-expressing (blue dots) females across three sessions. Two-way repeated measures ANOVA reveals no main effect of virus treatment $F_{1-29}=0.7892$, but significant effects of session $F_{2,58}=6.181$ ($p=0.0037$) and interaction $F_{2,58}=13.42$ ($p<0.0001$). Post-hoc analysis Bonferroni's multiple comparisons. k. Duration of parental behaviours displayed by control (open dots) and ChR2-expressing (blue dots) females. Two-way repeated measures ANOVA reveals no main effect of virus $F_{1-29}=2.721$ or session $F_{2,58}=1.178$, but a significant interaction effect $F_{2,58}=4.747$ ($p=0.0123$) followed by Tukey's post-hoc analysis. l. (left) Time spent in the nest with pups across three sessions in

18

control (open dots) versus ChR2 (blue dots) females. Two-way repeated measures ANOVA reveals no significant main effect of virus treatment F_{1-29}=1.637 or session $F_{2,58}$=0.6324, but a significant interaction effect $F_{2,58}$=3.746 (p=0.0295). Post-hoc analysis Tukey's multiple comparisons test. (right) Time spent in the nest with pups. Two-way repeated measures ANOVA shows a significant interaction effect $F_{2,58}$=3.746 (p<0.03). Post-hoc analysis by Tukey's multiple comparisons test. m. Number of females displaying parental behaviours across three sessions in control and ChR2 females (accelerated failure regression model with first session as time-point baseline and control as treatment baseline, significant difference between control and ChR2 females in second laser on session p<0.04). n. Number of females in control or ChR2 groups displaying aggressive behaviours toward pups. o. (left) Locomotion velocity in control or ChR2 females with or without laser stimulation is not significantly affected. (right) Aggression toward an adult castrated male intruder was unaffected. p. Setup for chemogenetic activation of PeFA^{Ucn3} neurons in virgin females. q. (left) Cumulative retrieval in cre+ (n=11) or cre- control (n=10) females. Kolmogorov-Smirnov test for significance p<0.0001. (right) Latency to retrieve first pup, Mann-Whitney test p=0.051. r. (Left) Number of females in Cre+ or Cre- (control) displaying parental behaviours. Significance determined by Fisher's exact test (p=0.0075). (right) Parental behaviours, t-test p<0.0291. s. (left) Duration in nest, Mann-Whitney test, p=0.0039. (right) Nest building, Mann-Whitney test p=0.0422. t. (left) Number of females in Cre+ or Cre - (control) displaying infant-directed aggression. (right) Investigation bout length.
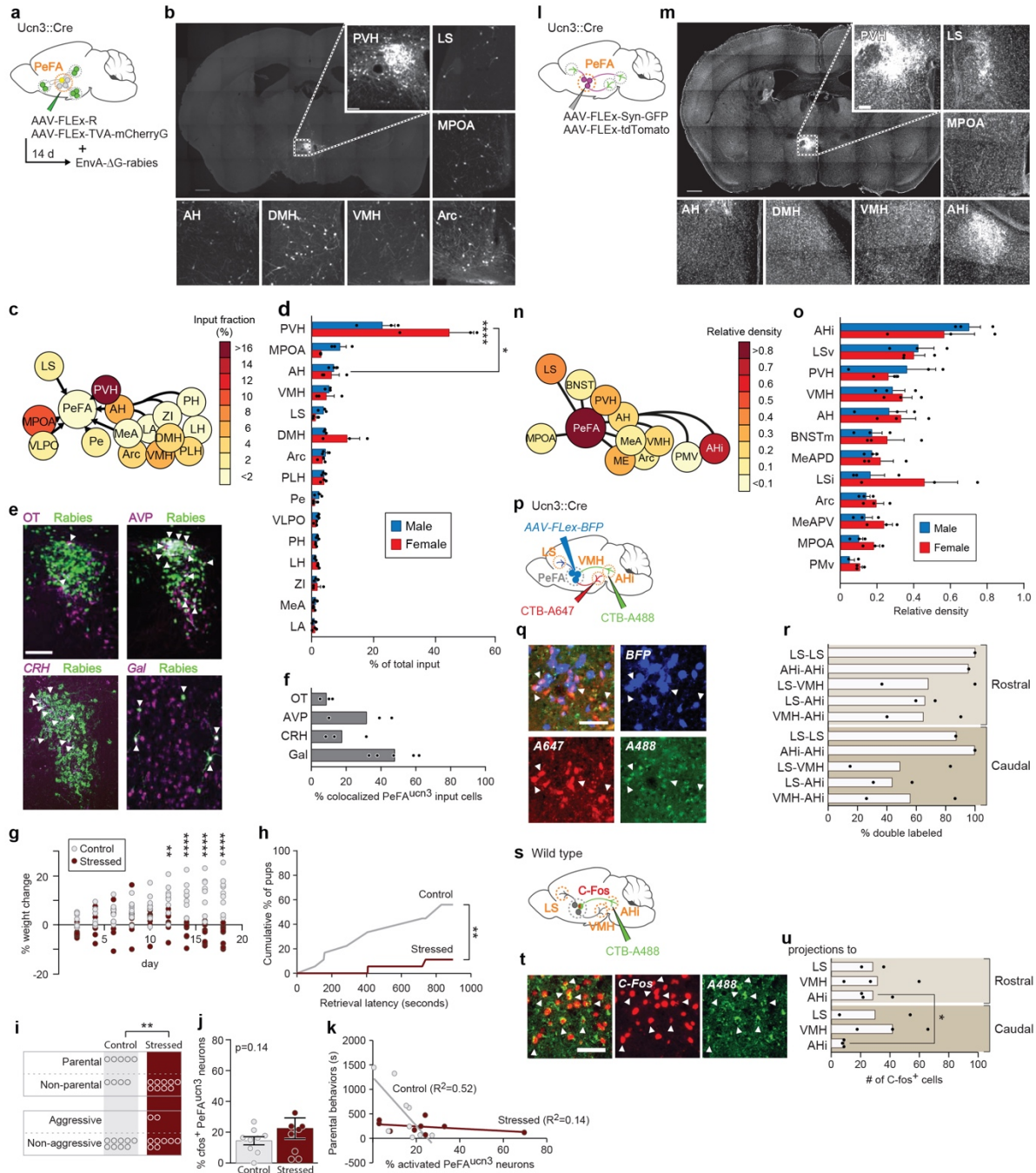
19

Figure 3. Inputs and output of PeFA^Ucn3 neurons and effect of stress.

a. Monosynaptic retrograde tracing from PeFA^Ucn3 neurons. b. Representative images of labeled monosynaptic inputs (scale bar 200 μm). c. Heatmap of input fractions by brain area in males. d. Quantification of input fraction in males (n=3) and females (n=3). Regions are ranked by effect size largest (top) to smallest (bottom) relative to values observed in males using a regression model and PVH, MPOA,

20

and AH showed significantly enriched levels of input to the PeFA^{Ucn3} neurons (p<0.0001), *post-hoc* test significant for PVH male vs. female). e. Representative images of immunofluorescence (OT, AVP) or in situ hybridization (CRH, *Gal*) co-staining with Rabies-GFP (scale bar, 200 µm). f. Percentages of presynaptic neurons expressing OT, AVP, CRH or Gal (n=3-5/group). g. Percentage of weight change in control (n=9) and stressed (n=9) females. Two-way repeated measures ANOVA, control versus stressed $F_{(1-16)}$=18.13, p<0.0006, days of stress $F_{(8,128)}$=8.366, p<0.0001, interaction $F_{(8,128)}$=16.69, p<0.0001, followed by Bonferroni's correction for multiple comparisons. h. Cumulative pup retrieval by control versus stressed females. Kolmogorov-Smirnov test p<0.0059. i. Number of females in control or stressed group showing parental (top panel) or aggressive (bottom panel) behaviours toward pups. Two-tailed Chi-square test significant (p<0.009). j. Percentage of *c-fos* positive *Ucn3* neurons in the PeFA of control and stressed females is not significantly different. k. Activation of PeFA^{Ucn3} neurons strongly correlates with cumulative parental behaviour in control females (R^2=0.52, significantly non-zero slope p<0.029) and this correlation is lost in stressed females (R^2=0.14, nonsignificant slope p<0.327). l. Anterograde tracing strategy. m. Representative images of synaptophysin densities in projection areas (scale bar 200 µm). n. Heatmap of relative densities of PeFA^{Ucn3} projections. o. Quantification of relative densities of PeFA^{Ucn3} projections in males (n=3) and females (n=3), regression analysis reveals significant enrichment of AHi, LSv, and PVH projections (p<0.0001). p. Schematic of retrograde CTB tracing combined with PeFA^{Ucn3} reporter virus. q. Representative image of CTB experiment (scale bar 100 µm). r. Quantification of double labeled *Ucn3* neurons. s. Schematic of CTB tracing combined with C-Fos staining in infanticidal males. t. Representative image of CTB-C-Fos data from AHi experiment. u. Quantification of number of C-Fos positive cells labeled with CTB from a given projection in the rostral and caudal PeFA (n=2-3/group). Rostral versus caudal percentages are significantly different for AHi-projecting neurons (paired t-test p<0.03).
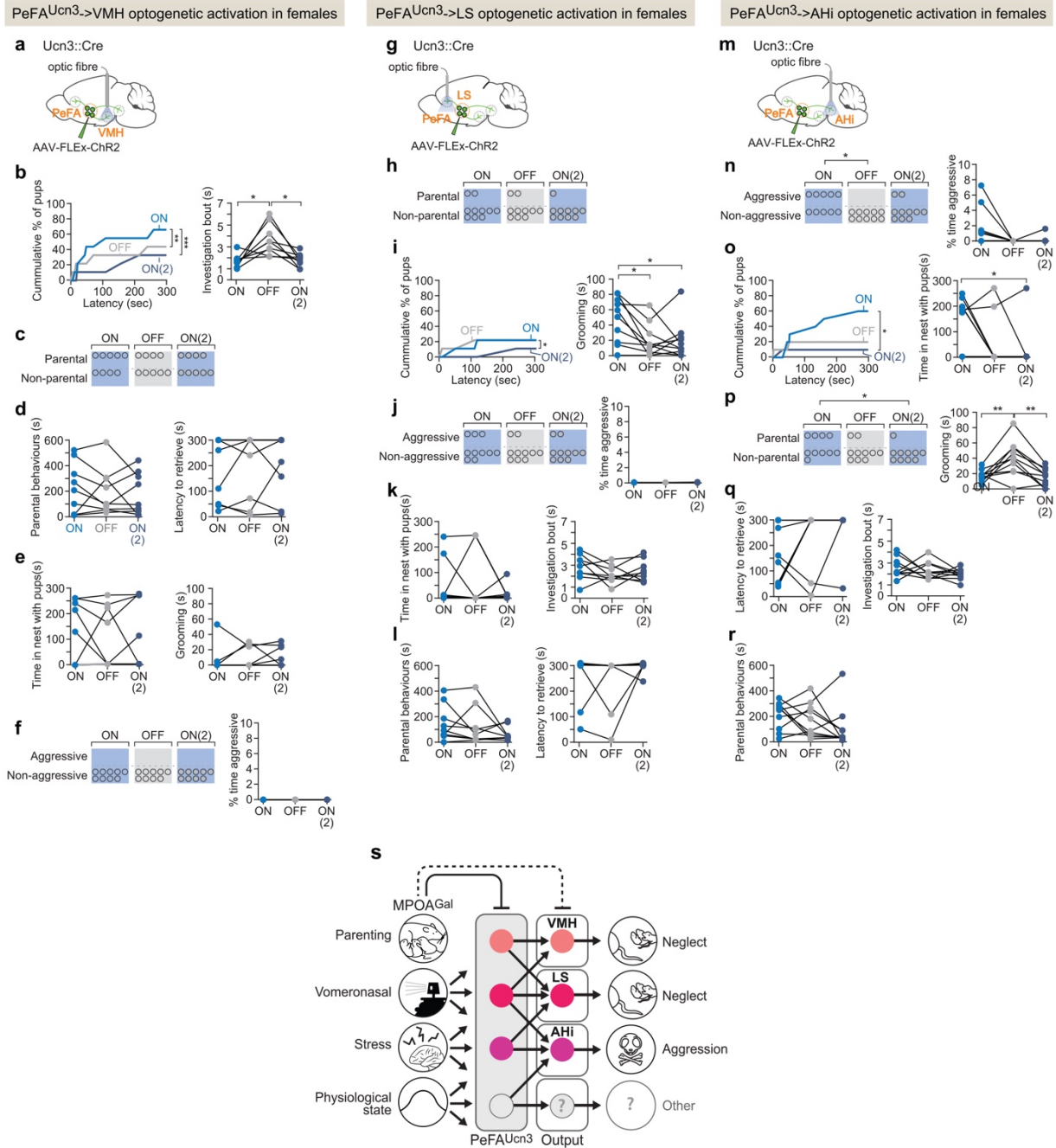
Figure 4. Specific projections from PeFA[Ucn3] neurons mediate infant-directed neglect and aggression.

a. Optogenetic stimulation of PeFA[Ucn3] to VMH fibre terminals. b. (left) Cumulative retrieval of pups is significantly different Friedman statistic $_{(3-15)}$ = 19.57, p<0.0001. Dunn's multiple comparisons test reveals difference between ON vs. ON2 (***) and OFF vs. ON2 (*). (right) One-way repeated measures ANOVA revealed a significant difference in investigation bout length $F_{(1, 11)}$=10.12 (p<0.005). Tukey's multiple

comparisons revealed differences between ON vs. OFF (*) and OFF vs. ON2 (*). c. Number of females showing parental behaviour. d. (left) Duration of parental behaviours and (right) latency to retrieve pups were not changed. e. (left) Time in the nest with pups and (right) grooming were not altered by PeFA^{Ucn3} to VMH fibre stimulation. f. (left) Number of females showing pup-directed aggression and (right) percent time displaying aggression show no differences across sessions. g. Optogenetic stimulation of PeFA^{Ucn3} to LS terminals. h. Number of females showing parental behaviour is not affected. i. (left) Cumulative retrieval of pups is suppressed and significantly affected over the course of the experiment analyzed by Friedman test, Friedman statistic $_{(3-7)}$= 10.21 (p<0.0041).   Dunn's multiple comparisons test reveals significant differences in OFF vs. ON2 comparison (*). (right) One-way repeated measures ANOVA reveals that grooming is significantly reduced over the course of the experiment $F_{(2-16)}$=6.368 (p<0.0102). Tukey's multiple comparisons test reveals significant differences between ON vs. OFF (*) and ON vs. ON2 (*). j. (left) Number of females showing aggression and (left) time spent aggressive toward pups is not changed. k. (left) Time in the nest and (right) investigation bout length are not affected.   l. (left) Parental behaviours and (right) latency to retrieve are unaffected. m. Schematic of optogenetic stimulation of PeFA^{Ucn3} to AHi terminal stimulation. n. (left) Number of females showing aggressive behaviours toward pups is significantly different between laser on and laser off groups (Chi-square test p<0.02). (right) Friedman test reveals a significant difference in the time spent aggressive over the course of the experiment Friedman statistic $_{(3,10)}$= 6.500 (p<0.0247).

 o. (left) Friedman test reveals that cumulative retrieval of pups is significantly affected Friedman statistic $_{(3-11)}$=8.688 (p<0.0095). Dunn's multiple comparisons shows significant differences between ON vs. ON2 (*). (right) Time spent in the nest with pups was significantly reduced between ON vs. ON2 conditions (Repeated measures ANOVA $F_{(2,14)}$=4.297 p<0.0351, followed by Tukey's post-hoc test).   p. (left) Number of females showing parental behaviours was significant reduced between ON v. ON2 conditions (Chi-square p<0.0191). (right) One-way repeated measures ANOVA revealed reversibly reduced grooming by stimulating of PeFA^{Ucn3} to AHi axonal terminals $F_{(2,18)}$=11.40 (p<0.0006). Tukey's multiple comparisons test showed differences between ON vs. OFF (**) and OFF vs. ON2 (**). q. (left) Latency to retrieve and (right) investigation bout length were unaffected.   r. Duration of parental behaviours was unchanged across sessions. s. Model of the function of PeFA^{Ucn3} neuronal population. PeFA^{Ucn3} neurons receive input from

23

the vomeronasal pathway, as well as brain areas involved in the regulation of stress, physiological state, and parenting. PeFA^{Ucn3} neurons send bifurcating processes to major projection targets including the AHi, LS, and VMH. Stimulation of these projections specifically impact pup-directed behaviour including aggression (AHi), and neglect (LS and VMH). Inhibitory MPOA^{Gal} neurons send input to PeFA^{Ucn3} neurons and to subsets of PeFA^{Ucn3} projection targets such as VMH and LS, likely ensuring the repression of agonistic interactions with infants when animals are in a parenting state.
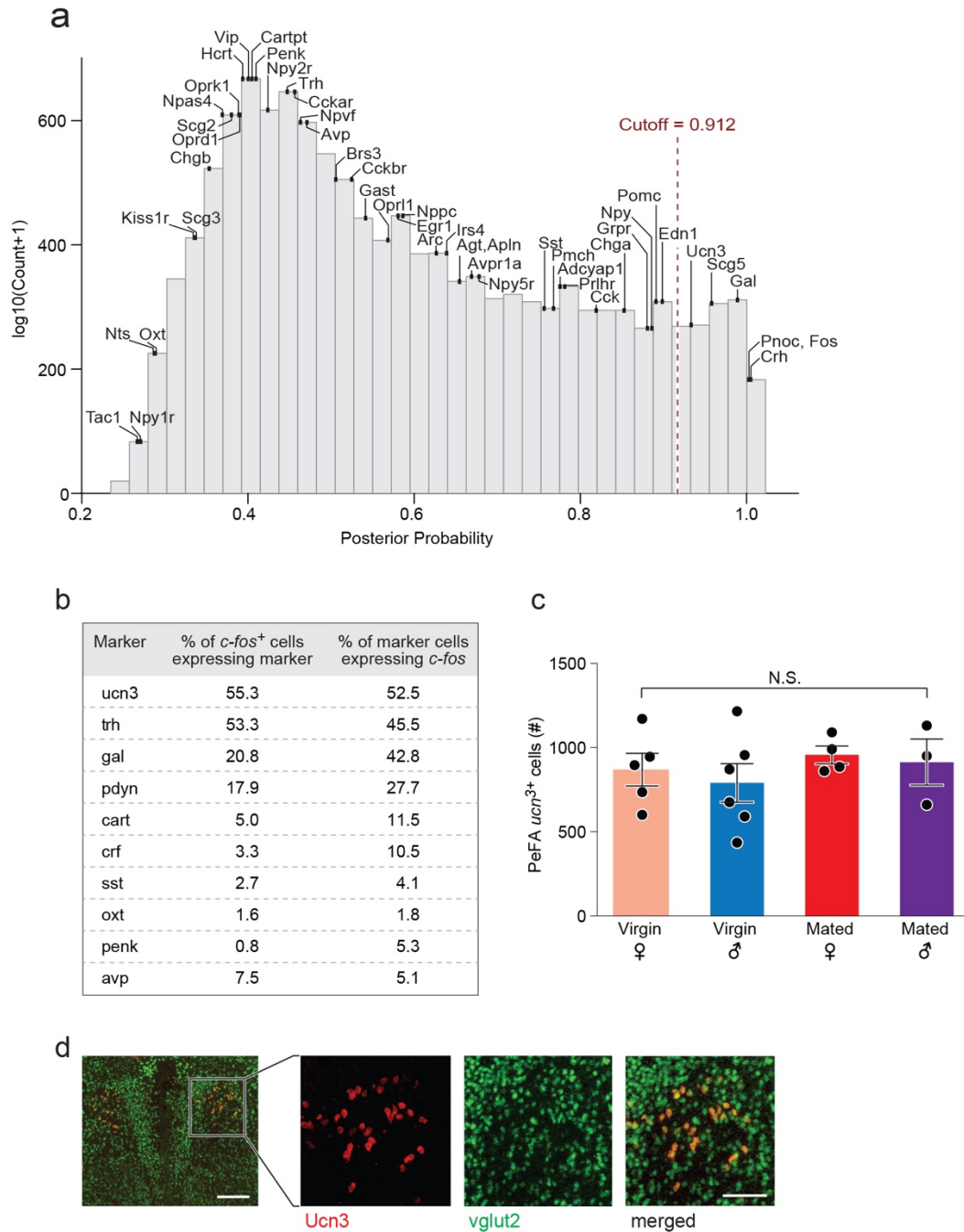
Supplemental figure 1. a. Distribution of the posterior probabilities of IP versus input expression levels being different in infanticidal males from that in naïve males. Vertical red-dashed line marks the empirically defined significant posterior-probability cutoff. Neuropeptides and their receptors are indicated corresponding to their posterior probabilities (n=3 biological replicates per group containing 10 pooled samples each). b. Table for expression levels of infanticide-induced *c-fos* and candidate marker genes in

the PeFA. c. *Ucn3* neurons in the PeFA compared among virgin and mated males and females reveals

no significant difference. d. Representative in situ hybridization images of *Ucn3* (red) colocalization with

vglut2 (green) in the PeFA (scale bar 100 μm).

26
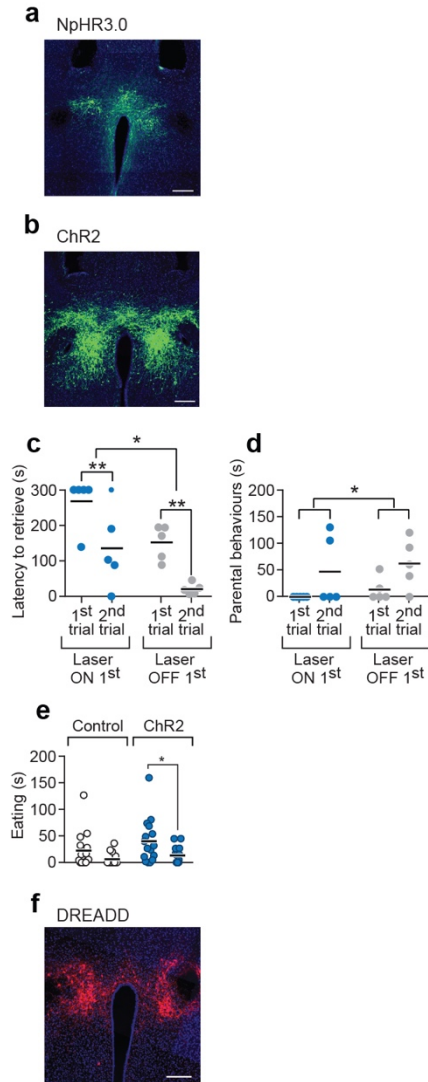
Supplemental figure 2. a. Representative image of halorhodopsin infection in the PeFA of Ucn3::cre males (scale bar 100 μm). b. Representative image of ChR2 infection in the PeFA of Ucn3::cre virgin females (scale bar 100 μm). c. Latency to retrieve pups in virgin females injected with ChR2 in either laser ON first conditions (blue dots; n=5) or laser OFF first conditions (gray dots; n=5). Two-way repeated measures ANOVA reveals a significant main effect of laser order ($F_{(1,8)}=8.235$ p<0.02 and session $F_{(1,8)}=39.16$ p<0.0002, Sidak's multiple comparisons test for on first condition and off first condition significant. d. Parental behaviour duration also showed a significant main effect of session ($F_{(1,8)}=6.519$, p<0.034 with no significant post-hoc effects. e. Eating duration of an appetitive food was significantly altered with laser treatment (two-way repeated measures ANOVA $F_{(1,29)}=8.504$, p<0.0068, Bonferroni's

27

multiple comparisons ON vs. OFF for ChR2 group) (n=15-16 per group).   f. Representative image of

DREADD virus infection in the PeFA of a Ucn3::cre virgin female (scale bar 100 μm).
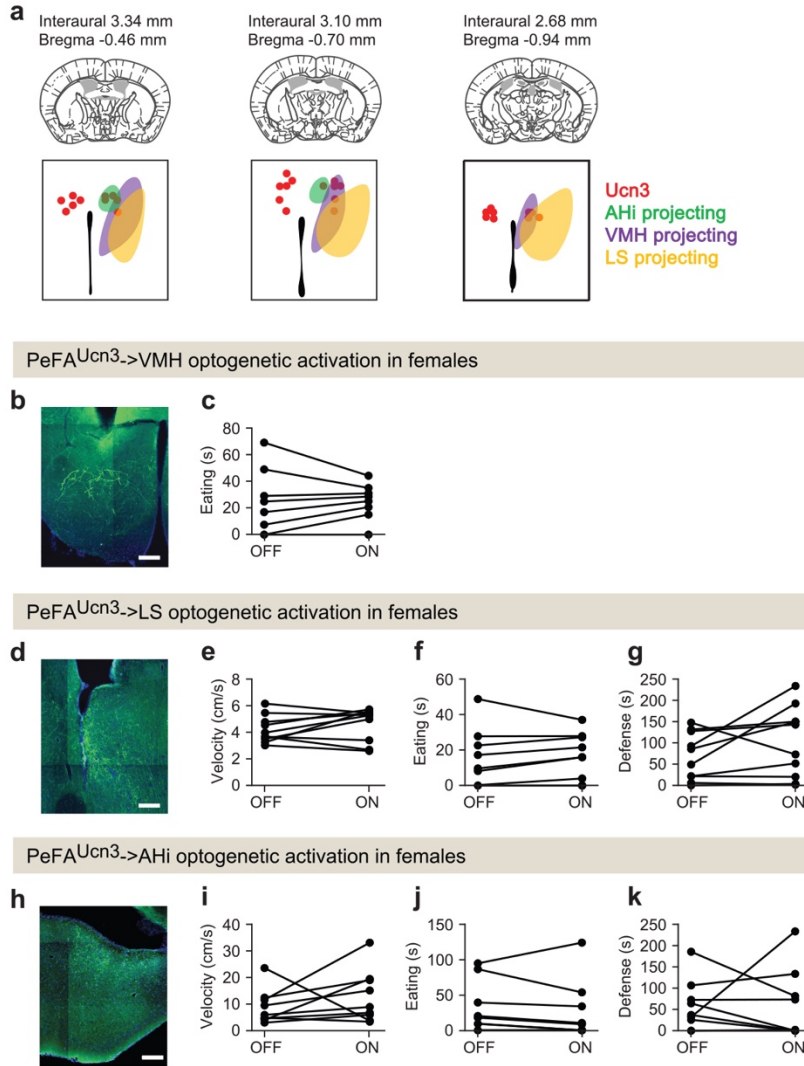
Supplemental figure 3. a. Schematic of projection targets of PeFA[ucn3] neurons. b. Representative image of ChR2 infection in Ucn3::cre virgin females with fibre implant directed toward the VMH, scale bar 100 μm. c. Time spent eating a cookie was not affected by laser condition (n=9). d. Representative image of ChR2 infection in Ucn3::cre virgin females with fibre implant directed toward the LS scale bar 100 μm. e. Velocity in locomotion test (n=9). f. Time spent eating a cookie (n=9). g. Time spent showing defensive behaviour toward a castrated male intruder swabbed with intact male urine (n=9). h. Representative image of ChR2 infection in Ucn3::cre virgin females with fibre implant directed toward the AHi, scale bar 100μm. i. Velocity in locomotion test (n=10). j. Time spent eating a cookie (n=10). k. Time spent showing defensive behaviour toward a castrated male intruder swabbed with intact male urine (n=10).

29

Supplemental Video 1. Virgin female with ChR2 expressed in PeFA[Ucn3] neurons shows tail rattling toward a pup intruder during laser stimulation of PeFA region.

Supplemental Video 2. Virgin female with ChR2 expressed in PeFA[Ucn3] neurons displays interruptions in investigation of a pup during laser stimulation of the ventromedial hypothalamus projections.

Supplemental Video 3. Virgin female with ChR2 expressed in PeFA[Ucn3] neurons shows abrupt escape-like behavior during laser stimulation of the lateral septum projections.

Supplemental Video 4. Virgin female with ChR2 expressed in PeFA[Ucn3] neurons shows aggressive carrying without retrieval typical of behavior displayed by infanticidal males during laser stimulation of amygdalohippocampal area projections.

METHODS

Animals

Mice were maintained on a 12h:12h dark light cycle with access to food and water ad libitum. All experiments were performed in accordance with NIH guidelines and approved by the Harvard University Institutional Animal Care and Use Committee (IACUC).

C57BL/6J mice as well as mice on a mixed C57BL/6J x 129/Sv background were used for the molecular identification of activated PeFA neurons.

The Ucn3::cre BAC transgenic line (STOCK Tg(Ucn3-cre) KF43Gsat/Mmcd 032078-UCD) was resuscitated from sperm provided by MMRRC. This line was generated by inserting a Cre-recombinase cassette followed by a polyadenylation sequence into a BAC clone at the initiating ATG codon of the first coding exon of the *Ucn3* gene. Sperm from the mixed B6/FVB male was introduced into oocytes from a B6/FVB female and the founding Cre+ animals were backcrossed to C57BL/6J. Mice from the F1 and F2 generations were used in experiments.

Behaviour assays

Mice were individually housed for at least 1 week prior to testing. Experiments were conducted during the dark phase under dim red light. Tests were recorded by Geovision surveillance system or by Microsoft LifeCam HD-5000 and behaviours were scored by an observed blind to experimental condition using Observer XT11 Software or Ethovision XT 8.0 (Noldus Information Technology). Animals were tested for a single behaviour per session with at least 24 hours between sessions.

Parental behaviour

Parental behaviour tests were conducted in the mouse's home cage as previously described[11,13]. Mice were habituated to the testing environment for 10 minutes. One to two C57BL6/J pups 1-4 days old were presented in the cage in the opposite corner to the nest. Test sessions began when the mouse first closely investigated a pup (touched the pup with its snout) and lasted for 5-15 minutes. In the event that the mouse became aggressive by biting and wounding the pup, the

31

session was immediately halted and the pup was euthanized. The following behaviours were quantified: latency to retrieve, sniffing (close contact), grooming (handling with forepaws and licking), nest building, time spent in the nest, crouching, latency to attack (latency to bite and wound), aggression (roughly handling, aggressively grooming, aggressive carrying with no retrieval), and tail rattling. A 'parenting behaviour' index was calculated as the sum of duration of sniffing, grooming, nest building, time spent in the nest, and crouching. Mice were categorized as 'parental' if they showed pup-retrieval behaviour and 'non-parental' if they did not retrieve pups. Mice were categorized as 'aggressive' if they showed bite attacks, tail rattling, aggressive pup carrying, or aggressive pup-grooming and 'non-aggressive' if they did not display any of these behaviours. Optogenetic experiments were limited to 5 minutes as previously performed for infanticidal testing, thus limiting the ability to score male retrieving behaviour which is typically displayed between 4 and 7 minutes[11,13]. Chemogenetic experiments lasted 15 minutes.

Conspecific aggression

Conspecific aggression assays were performed as previously described[30]. Briefly, castrated males were swabbed with ~40 µL of urine from an intact male and introduced into the home cage of the test mouse for 5 minutes (session started at first close contact).

Locomotor behaviour

Locomotor behaviour assays were performed in a 36 x 25 cm empty cage. Velocity and distance moved were tracked for 5 minutes.

Feeding behaviour

Feeding behaviour was assessed by introducing a small piece of palatable food (chocolate chip cookie) into the far corner of a mouse's home cage. Session started when mouse approached the food and behaviour was recorded for 5 minutes. Parameters rated were duration sniffing and eating the cookie.

Fluorescence in situ hybridization

32

Fluorescence *in situ* hybridization (FISH) was performed as previously described[13,53]. Briefly, fresh brain tissue was collected from animals housed in their home cage or 35 min after the start of the behaviour tests for immediate early gene (*c-fos*) studies. Only animals that engaged in a particular behaviour were used. Brains were embedded in OCT (Tissue-Tek) and frozen with dry ice. 20µm cryosections were used for mRNA in situ. Adjacent sections from each brain were collected over replicate slides to stain with multiple probes. The staining procedure is as previously described[13,53]. Complementary DNA of *c-fos, Ucn3, Gal, Crf, Trh, Pdyn, Cart, Sst, Oxt, Penk, Avp, and Yfp* were cloned in approximately 800-1200 base pairs (when possible) segments into pCRII-TOPO vector (Invitrogen). Antisense complementary RNA (cRNA) probes were synthesized with T7 or Sp6 (Promega) and labelled with digoxigenin (DIG; Roche) or fluorescein (FITC, Roche). Where necessary, a cocktail of 2 probes was generated covering different segments of the target sequence to increase signal to noise ratio.

Probe hybridization was performed with 0.5-1.0 ng/l cRNA probes in an oven at 68° C. Probes were detected by horseradish peroxidase (POD)-conjugated antibodies (anti-FITC-POD at 1/250 dilution, Roche; anti-DIG-POD at 1/500 dilution, Roche). Signals were amplified by biotin-conjugated tyramide (PerkinElmer) and visualized with Alexa Fluor-488-conjugated streptavidin or Alexa Fluor 568-conjugated streptavidin (Invitrogen), or directly visualized with TSA plus cyanine 3 system, TSA plus cyanine 5 system, or TSA plus Fluorescein system (PerkinElmer). Slides were mouted with Vectashield with 4',6-diamidino-2-phenylindole (DAPI, Vector Labs).

Laser-capture microscopy and microarray analysis

Males were sacrificed 35 minutes after onset of attacking behaviour for peak *c-fos* expression and fresh brain tissue was frozen in OCT. 20µm sections with alignment holes punched into the tissue by a glass pipet were prepared in a series with every other section collected on superfrost plus slides for in situ hybridization and the other for laser capture microdissection and collected on PEN coated membrane slides (Leica). Double fluorescence *in situ* hybridization (FISH) for *c-fos* and *oxytocin* was performed as previously described[13,53]. Sections prepared for laser-capture

33

were dehydrated and stained in a 50% ethanol solution containing cressyl violet. Using a Zeiss PALM microscope, slides from adjacent FISH and laser-capture sections are aligned via tissue pinches using PALM Software (Zeiss). After alignment, tissue from the area containing *c-fos*+, oxytocin+ cells, and an outside region were identified from FISH sections and collected from fresh laser sections by laser capture. For each region, tissue from 6 brains were pooled to prepare total RNA (RNEasy micro kit, Qiagen) for reverse transcription and amplification to cDNA (Ovation Pico WTA kit, Nugen). Three biological replicates of cDNA (n=18 total brain samples; 6 pooled per replicate) were prepared for hybridization to the Affymetrix Exon ST 1.0 array as described by the manufacturer. Differential expression analysis was performed using the Affymetrix Expression Console software to analyze gene expression levels. We then performed a paired t-test to determine genes with significantly altered gene expression in the *c-fos*+ area compared to bordering cell regions. Finally, in order to rank genes taking into account the fold change and expression level, we performed a residual analysis on the regression (Fig. 1d) and found that *Avp* and *Ucn3* had the highest residual values (*Avp* 5.66, *Ucn3* 4.80).

pS6 pulldowns and RNAseq analysis

Adult male mice were habituated in their home cages to a testing room for 4 hours. Males were then either presented with a 1-4 day old C57BL/6J pup or no stimulus and allowed to interact for 10 minutes, after which time behaviour was recorded and the pup was removed. Sixty minutes after stimulus presentation, males were sacrificied and a punch (1 mm diameter) was collected from a 2mm thick brain slice containing the perifornical area, the paraventricular nucleus, and part of the anterior hypothalamus. The tissue was processed for pS6 immunoprecipitation as described previously[15]. Briefly, punches were held in (ice-cold homogenization buffer (10mM HEPES, 150mM KCl, 5mM MgCl2 and containing 1X phosphatase inhibitor cocktail, 1X Calyculin. Protease inhibitor cocktail (EDTA free), 250ug/ml Cycloxeximide and 2.5ul/ml Rnasin) and 10 punches were pooled per sample, with 3 biological replicates taken from infanticidal and naïve groups. Tissue was homogenized, centrifuged for 10 minutes at 2000 g, subjected to treatment

34

with 0.7% NP40 and 20mM DHPC and centrifuged for 10 minutes at (20,000rcf) at 4° C to obtain the supernatant containing the input fraction. A (10 µL sample) of the input was kept for sequencing and the remaining input fraction was incubated with Protein A Dynabeads (Invitrogen) conjugated to pS6 antibody (Life Technologies 44923G) at a concentration of around 4 µg/IP for 10 minutes at 4° C. Beads were collected on a magnet and washed in 0.15M KCl wash buffer, then associated RNAs were lysed into RLT buffer and RNA was isolated using the RNAeasy Micro kit (Qiagen) according to manufacturer's instructions. RNA was checked for quality and quantity on an Agilent tape station. High quality samples from matched input and IP fractions were prepared using the (Low-input Library Prep kit (Clontech).

Sequenced reads were mapped with STAR aligner[54], version 2.5.3a, to the mm10 reference mouse genome and the Gencode vM12 primary assembly annotation[55], to which non-redundant UCSC transcripts were added, using the two-round mapping approach. This means that following a first mapping round of each library, the splice-junction coordinates reported by STAR, across all libraries, are fed as input to the second round of mapping. The parameters used in both mapping rounds are: outSAMprimaryFlag ="AllBestScore", outFilterMultimapNmax="10", outFilterMismatchNoverLmax="0.05", outFilterIntronMotifs="RemoveNoncanonical". Following read mapping, transcript and gene expression levels were estimated using MMSEQ[56]. Following that transcripts and genes which cannot be distinguished according to the read data were collapsed using the mmcollapse utility of MMDIFF[57], and the Fragments Per Killobase Million (FPKM) expression units were converted to natural logarithm of Transcript Per Million (TPM) units since the latter were shown to be less biased and more interpretable[58]. In order to test for differential gene activation between the infanticidal males and naïve males, we used a Bayesian regression model[59]. We defined the response (for each transcript or gene) as the difference between means of the posterior TPMs of the IP and input samples (i.e., paired according to the tissue punches from which they were obtained). The uncertainty in the response was computed as square root of the sum of the variances of the posterior TPMs of the IP and input samples

35

divided by the number of posterior samples (1,000). The categorical factor for which we estimated the effect was defined as the behaviour of the animal, meaning infanticidal and naïve, where naïve was defined as baseline. Hence, our Bayesian regression model estimates the posterior probability of the natural logarithm of the ratio between infanticidal IP TPMs divided by input TPMs and naive IP TPMs divided by input TPMs being different from zero. In order to define a cutoff of this posterior probability, above which we consider the activation (i.e. effect size) significant, we searched for a right mode in the distributions of posterior probabilities across all transcripts and genes (separately for each), and placed the cutoff at the local minima that separates the right mode from the left mode, which represents transcripts and genes for which the likelihood of differential gene activation is very weak and hence their posterior probability is dominated by the prior (Supp. Fig. S1a).

Optogenetics

Ucn3::Cre mice 8-12 weeks old were used for these experiments. Pilot experiments and our previous observations indicated that mated parents were insensitive to manipulations aimed at reducing parental behaviours[13], so we used virgin males and females in order to maximize our opportunity to see decrements in parenting. Virgin males were prescreened for infanticidal behaviour. We injected 200 nL of AAV1/DIO-hChR2-eYFP for activation or AAV1/FLEx-NpHR3.0-eYFP for inhibition (or AAV1/FLEx-YFP or AAV1/FLEx-tdTomato as control virus) bilaterally into the perifornical area (AP -0.6, ML ±0.3, DV -4.2). Mice recovered for 1-2 weeks and in a second surgery a dual fibre optic cannula (300 μm, 0.22 NA, Doric Lenses) was implanted 0.5 mm above the target area and affixed to the skull using dental cement. Cannula positions were as follows: PeFA = AP -0.6mm, ML ± 0.5mm, DV -3.7mm; LS = AP 0.3mm ML ± 0.5mm DV -3.2mm; VMH= AP ML ± 0.5mm DV; AHi = AP -2.3mm, ML ± 2.5mm, DV -4.7mm. Mice recovered for an additional week prior to the start of behavioural testing. In pilot studies we found that order of testing impacted parental behaviour results, so rather than randomizing test order, we

36

alternated laser on and off conditions in the same order for both control and manipulated mice. For locomotion, feeding, and conspecific aggression tests, we randomized the order of laser on/off presentation. On test days, the fibre implant was connected to an optical fibre with commutator connected to either a 473 nm laser (150 mW, Laserglow Technologies), or a 460 nm LED (50W, Prizmatix) for ChR2 stimulation, or to a 589 nm laser (300mW, OptoEngine) for NpHR3.0 inhibition. Behaviour tests were 5 minutes in duration for each condition and behaviour category. For parental behaviour assays with ChR2, the 473 nm laser or 460 nm LED was triggered in 20ms pulses at 20 Hz for 2 seconds when the mouse contacted the pup with its snout, and the order of laser sessions was on first, off second, on third. For locomotor experiments with ChR2 activation, the laser was triggered (20ms, 20 Hz, 2 seconds) every 10 seconds to approximately equivalent duration as the time laser was on during the parental sessions. For cookie experiments with activation, the laser was triggered when the mouse contacted the cookie. For conspecific aggression experiments with activation, the laser was triggered when the test mouse made close contact with the intruder mouse. The power exiting the fibre tip was 5mW, which translates to ~2 mW/mm^2 at the target region (calculator provided by Deissertoth lab at http://www.stanford.edu/group/dlab/cgi-bin/graph/chart.php). For all behaviour assays with NpHR3.0, the 589 nm laser was illuminated (20 ms, 50 Hz) throughout the duration of the 5 minute session at a power of 15 mW, or ~8.4 mW/mm^2. For parenting sessions with inhibition, the order of laser sessions was off first, on second, off third.

Chemogenetics

Ucn3::Cre virgin female mice (or cre negative littermates as controls) 8-12 weeks old were used for these experiments. We injected 200 nL of AAV1/DIO-hM3Dq virus bilaterally into the PeFA (AP -0.6mm, ±ML 0.3mm, DV -4.2mm). Mice recovered for two weeks prior to behaviour testing. Cre positive and cre negative females were administered 0.3mg/kg clozapine-*n*-oxide dissolved in saline intraperitoneally and habituated to the testing environment for 30 minutes. Females

37

were presented two C57BL6/J pups in the corner of their homecage opposite the nest and parental behaviours were recorded for 15 minutes.

Anterograde tracing

AAV2.1-FLEX-tdTomato virus (UPenn Vector Core) and AAV2.1-FLEX-synaptophysin-eGFP virus (plasmid gift of Dr. Silvia Arber; custom virus prep, UNC Vector Core) were mixed at a ratio of 1:2 and stereotaxically injected unilaterally into the PeFA (Bregma coordinates AP: -0.6mm; ML: -0.3mm; DV: -4.2mm) using a Drummond Nanoject II (180 nL to cover entire structure) into adult virgin male (n=3) and female (n=3) Ucn3::cre mice. After 2 weeks, mice were transcardially perfused with 4% paraformaldehyde. Tissue was cryoprotected (30% sucrose) and serial sections were prepared on a freezing microtome (60 µm). Every third section was immunostained using Anti-GFP antibody (described in immunohistochemistry methods), mounted to superfrost plus slides, coverslipped with Vectashield plus DAPI and imaged at 10X magnification using the AxioScan (Zeiss). Synaptic densities were quantified by ImageJ software after background subtraction and a density ratio was prepared by dividing by the density at the injection site which was normalized to 100%. Density ratio was compared across brain regions by One-way ANOVA followed by Dunnett's test for multiple comparisons and sexual dimorphisms compared using a two-tailed t-test.

Retrograde tracing with CTB

Retrograde tracing was performed in either Ucn3::Cre males aged 8-12 weeks injected into the PeFA bilaterally with AAV1/FLEx-BFP allowed to recover for 10 days, or into C57BL6/J males aged 8 weeks prescreened for infanticide. In Ucn3::Cre males, pairwise injections of 80 nL of 0.5% (wt/vol) fluorescently labeled cholera toxin B subunit (CTB-488, ThermoFisher C22841, CTB-647, ThermoFisher C34788). In C57BL6/J mice, only CTB-488 was injected. After 7 days, Ucn3::Cre mice were transcardially perfused and brains were postfixed overnight, cryoprotected in 30% sucrose overnight, and 60 µm sections were prepared on a sliding microtome. Sections were imaged at 10X (Axioscan, Zeiss) and the fraction of BFP+ cells double-labeled with CTB-

38

488 and CTB-647 was quantified. In control experiments, a 1:1 mixture of CTB-488 and CTB-647 was injected into the LS and AHi. In C57BL6/J mice, males were habituated to a testing environment for two hours then presented with one foreign C57BL6/J pup in the far corner of their homecage. When the male attacked the pup, the pup was removed from the cage and euthanized. Males were perfused 80-90 minutes after pup exposure and brains were postfixed overnight, cryoprotected in 30% sucrose overnight, and 60 μm sections were prepared on a sliding microtome. Tissue was stained with C-Fos antibody (see details in immunostaining section), imaged at 10X (Axioscan, Zeiss), and the number of C-Fos positive cells labeled with CTB-488 was quantified.

Monosynaptic input tracing

A 1:1 ratio (180 nL to cover the entire region) of AAV2.1-FLEx-TVA-mCherry (avian TVA receptor) and AAV2.1-FLEx-RG (rabies glycoprotein) was stereotaxically injected unilaterally into the PeFA (Bregma coordinates AP: -0.6mm; ML: 0.3mm; DV: -4.2mm) of adult Ucn3::cre male and female mice (n=3/sex). Two weeks later, g-deleted rabies virus (deltaG-RV-eGFP) (300 nL) was injected into the same coordinate. Seven days later, mice were transcardially perfused with 4% paraformaldehyde. Tissue was postfixed in PFA overnight and cryoprotected (30% sucrose) then serial sections were prepared on a freezing microtome (60 μm). Every third section was imaged at 10X using the AxioScan (Zeiss). Cell bodies labeled by eGFP in anatomical areas were quantified and an input ratio was prepared by dividing the number of input cells in each region by the total number of input cells in each brain. Input ratio was compared across brain regions by One-way ANOVA followed by Dunnett's test for multiple comparisons and sexual dimorphisms compared using a two-tailed t-test.

Immunohistochemistry

C-Fos antibody staining

To visualize C-Fos protein in combination with CTB, perfused tissue was sliced on a freezing microtome at 30 μm, and every 3rd section throughout the perifornical area was stained. Briefly,

39

sections were rinsed in PBS with 0.1% Triton (PBST), then blocked in 2% normal horse serum and 3% fetal bovine serum diluted in PBST for 2 hours at room temperature. Primary antibody Rabbit anti-C-Fos (Synaptic Systems) was diluted 1:2000 in PBS and sections were incubated for 72 hours at 4°C. After rinsing with PBST, secondary Anti-Rabbit A568 (1:1000) was applied at 1:1000 dilution in PBS for 48 hours at 4° C. Sections were rinsed in PBS, mounted to superfrost plus slides, coverslipped with Vectashield containing DAPI, and imaged (see details above).

GFP antibody staining

To amplify synaptophysin densities in the anterograde tracing experiments, the GFP signal was enhanced by antibody staining. Perfused tissue was sliced on a freezing microtome at 60 μm, and every 3rd section throughout the brain was stained. Briefly, sections were rinsed in PBS with 0.1% Triton (PBST), then blocked in 1.5% normal horse serum diluted in PBST for 1 hour (blocking solution) at room temperature. Primary antibody Rabbit anti-GFP (Novus Biologicals NB600-308) was diluted 1:2000 in blocking solution and sections were incubated overnight at 4° C. After rinsing with PBST, secondary anti-Rabbit-A488 was applied at 1:200 dilution in blocking buffer and incubated overnight at 4° C. Sections were rinsed in PBS, mounted to superfrost plus slides, coverslipped with Vectashield containing DAPI, and imaged (see details above).

Oxytocin/vasopressin staining

Perfused tissue was sliced on a sliding microtome at 60 μm. Every 3rd section from the perifornical area was stained. Briefly, sections were rinsed in PBS with 0.1% Triton (PBST), then blocked in 10% fetal bovine serum diluted in PBST. Primary antibody Rabbit anti-vasopressin (Immunostar) or Rabbit anti-oxytocin (Millipore) were diluted 1:1000 in PBST and sections were incubated overnight at 4° C. After rinsing with PBST, secondary anti-Rabbit A647 was applied at 1:200 dilution in blocking buffer and incubated overnight at 4° C. Sections were rinsed in PBS, mounted to superfrost plus slides, coverslipped with Vectashield containing DAPI, and imaged on the Axioscan (Zeiss) at 10X magnification.

40

41

REFERENCES

1   Hrdy, S. B. Male-male competition and infanticide among the langurs (Presbytis entellus) of Abu, Rajasthan. *Folia Primatol (Basel)* **22**, 19-58, doi:10.1159/000155616 (1974).

2   Hrdy, S. B. Infanticide among animals: A review, classification, and examination of the implications for the reproductive strategy of females. *Ethology and Sociobiology* **1**, 13-40 (1979).

3   Parmigiani, S. & Vom Saal, F. S. *Infanticide and parental care*. (Harwood Academic Publishers, 1994).

4   Heasley, J. E. Energy Allocation in Response to Reduced Food Intake in Pregnant and Lactating Laboratory Mice. *Acta Theriologica* **28**, 55-71 (1983).

5   König, B. Behavioural ecology of kin recognition in house mice. *Ethology Ecology & Evolution* **1**, 99-110, doi:10.1080/08927014.1989.9525534 (1989).

6   Marsteller, F. A. & Lynch, C. B. Reproductive responses to variation in temperature and food supply by house mice: II. Lactation. *Biol Reprod* **37**, 844-850, doi:10.1095/biolreprod37.4.844 (1987).

7   Svare, B., Bartke, A. Food deprivation induces conspecific killing in mice. *Aggressive Behavior* **4**, 253-261 (1978).

8   Lukas, D. & Huchard, E. The evolution of infanticide by females in mammals. *bioRxiv*, 405688, doi:10.1101/405688 (2018).

9   Hillerer, K. M., Neumann, I. D. & Slattery, D. A. From stress to postpartum mood and anxiety disorders: how chronic peripartum stress can impair maternal adaptations. *Neuroendocrinology* **95**, 22-38, doi:10.1159/000330445 (2012).

10   Fang, Y. Y., Yamaguchi, T., Song, S. C., Tritsch, N. X. & Lin, D. A Hypothalamic Midbrain Pathway Essential for Driving Maternal Behaviors. *Neuron* **98**, 192-207 e110, doi:10.1016/j.neuron.2018.02.019 (2018).

11   Kohl, J. *et al.* Functional circuit architecture underlying parental behaviour. *Nature* **556**, 326-331, doi:10.1038/s41586-018-0027-0 (2018).

12   Marlin, B. J., Mitre, M., D'Amour J, A., Chao, M. V. & Froemke, R. C. Oxytocin enables maternal behaviour by balancing cortical inhibition. *Nature* **520**, 499-504, doi:10.1038/nature14402 (2015).

13   Wu, Z., Autry, A. E., Bergan, J. F., Watabe-Uchida, M. & Dulac, C. G. Galanin neurons in the medial preoptic area govern parental behaviour. *Nature* **509**, 325-330, doi:10.1038/nature13307 (2014).

14   Kohl, J., Autry, A. E. & Dulac, C. The neurobiology of parenting: A neural circuit perspective. *Bioessays* **39**, 1-11, doi:10.1002/bies.201600159 (2017).

15   Knight, Z. A. *et al.* Molecular profiling of activated neurons by phosphorylated ribosome capture. *Cell* **151**, 1126-1137, doi:10.1016/j.cell.2012.10.039 (2012).

16   Lonstein, J. S. & De Vries, G. J. Sex differences in the parental behavior of rodents. *Neurosci Biobehav Rev* **24**, 669-686 (2000).

17   Fekete, E. M. *et al.* Delayed satiety-like actions and altered feeding microstructure by a selective type 2 corticotropin-releasing factor agonist in rats: intra-hypothalamic urocortin 3 administration reduces food intake by prolonging the post-meal interval. *Neuropsychopharmacology* **32**, 1052-1068, doi:10.1038/sj.npp.1301214 (2007).

18   Jamieson, P. M. *et al.* Urocortin 3 transgenic mice exhibit a metabolically favourable phenotype resisting obesity and hyperglycaemia on a high-fat diet. *Diabetologia* **54**, 2392-2403, doi:10.1007/s00125-011-2205-6 (2011).

19   Wickersham, I. R. *et al.* Monosynaptic restriction of transsynaptic tracing from single, genetically targeted neurons. *Neuron* **53**, 639-647, doi:10.1016/j.neuron.2007.01.033 (2007).

42

20   Donaldson, Z. R. & Young, L. J. Oxytocin, vasopressin, and the neurogenetics of sociality. *Science* **322**, 900-904, doi:10.1126/science.1158668 (2008).

21   Insel, T. R. The challenge of translation in social neuroscience: a review of oxytocin, vasopressin, and affiliative behavior. *Neuron* **65**, 768-779, doi:10.1016/j.neuron.2010.03.005 (2010).

22   Jezova, D., Skultetyova, I., Tokarev, D. I., Bakos, P. & Vigas, M. Vasopressin and oxytocin in stress. *Ann N Y Acad Sci* **771**, 192-203 (1995).

23   Swanson, L. W. & Sawchenko, P. E. Paraventricular nucleus: a site for the integration of neuroendocrine and autonomic mechanisms. *Neuroendocrinology* **31**, 410-417, doi:10.1159/000123111 (1980).

24   Jeong, J. Y., Lee, D. H. & Kang, S. S. Effects of chronic restraint stress on body weight, food intake, and hypothalamic gene expressions in mice. *Endocrinol Metab (Seoul)* **28**, 288-296, doi:10.3803/EnM.2013.28.4.288 (2013).

25   Maestripieri, D., Badiani, A. & Puglisi-Allegra, S. Prepartal chronic stress increases anxiety and decreases aggression in lactating female mice. *Behavioral neuroscience* **105**, 663-668 (1991).

26   Albert, D. J. & Chew, G. L. The septal forebrain and the inhibitory modulation of attack and defense in the rat. A review. *Behav Neural Biol* **30**, 357-388 (1980).

27   Anthony, T. E. *et al.* Control of stress-induced persistent anxiety by an extra-amygdala septohypothalamic circuit. *Cell* **156**, 522-536, doi:10.1016/j.cell.2013.12.040 (2014).

28   Blanchard, D. C., Blanchard, R. J., Takahashi, L. K. & Takahashi, T. Septal lesions and aggressive behavior. *Behav Biol* **21**, 157-161 (1977).

29   Canteras, N. S., Chiavegatto, S., Ribeiro do Valle, L. E. & Swanson, L. W. Severe reduction of rat defensive behavior to a predator by discrete hypothalamic chemical lesions. *Brain Res Bull* **44**, 297-305 (1997).

30   Kruk, M. R. *et al.* Discriminant analysis of the localization of aggression-inducing electrode placements in the hypothalamus of male rats. *Brain research* **260**, 61-79 (1983).

31   Lee, H. *et al.* Scalable control of mounting and attack by Esr1+ neurons in the ventromedial hypothalamus. *Nature* **509**, 627-632, doi:10.1038/nature13169 (2014).

32   Lin, D. *et al.* Functional identification of an aggression locus in the mouse hypothalamus. *Nature* **470**, 221-226, doi:10.1038/nature09736 (2011).

33   Slotnick, B. M., McMullen, M. F. & Fleischer, S. Changes in emotionality following destruction of the septal area in albino mice. *Brain Behav Evol* **8**, 241-252, doi:10.1159/000124357 (1973).

34   Dulac, C., O'Connell, L. A. & Wu, Z. Neural control of maternal and paternal behaviors. *Science* **345**, 765-770, doi:10.1126/science.1253291 (2014).

35   Amano, T. *et al.* Development-dependent behavioral change toward pups and synaptic transmission in the rhomboid nucleus of the bed nucleus of the stria terminalis. *Behav Brain Res* **325**, 131-137, doi:10.1016/j.bbr.2016.10.029 (2017).

36   Fleming, A. S. & Rosenblatt, J. S. Olfactory regulation of maternal behavior in rats. I. Effects of olfactory bulb removal in experienced and inexperienced lactating and cycling females. *Journal of comparative and physiological psychology* **86**, 221-232 (1974).

37   Fleming, A. S. & Rosenblatt, J. S. Olfactory regulation of maternal behavior in rats. II. Effects of peripherally induced anosmia and lesions of the lateral olfactory tract in pup-induced virgins. *Journal of comparative and physiological psychology* **86**, 233-246 (1974).

38   Fleming, A. S., Vaccarino, F. & Luebke, C. Amygdaloid inhibition of maternal behavior in the nulliparous female rat. *Physiology & behavior* **25**, 731-743 (1980).

39   Gammie, S. C. & Nelson, R. J. cFOS and pCREB activation and maternal aggression in mice. *Brain research* **898**, 232-241 (2001).

40   Isogai, Y. *et al.* Multisensory Logic of Infant-Directed Aggression by Males. *Cell* **175**, 1827-1841 e1817, doi:10.1016/j.cell.2018.11.032 (2018).

43

41   Deussing, J. M. *et al.* Urocortin 3 modulates social discrimination abilities via corticotropin-releasing hormone receptor type 2. *The Journal of neuroscience : the official journal of the Society for Neuroscience* **30**, 9103-9116, doi:10.1523/JNEUROSCI.1049-10.2010 (2010).

42   Kuperman, Y. *et al.* Perifornical Urocortin-3 mediates the link between stress-induced anxiety and energy homeostasis. *Proc Natl Acad Sci U S A* **107**, 8393-8398, doi:10.1073/pnas.1003969107 (2010).

43   Venihaki, M. *et al.* Urocortin III, a brain neuropeptide of the corticotropin-releasing hormone family: modulation by stress and attenuation of some anxiety-like behaviours. *J Neuroendocrinol* **16**, 411-422, doi:10.1111/j.1365-2826.2004.01170.x (2004).

44   Tachikawa, K. S., Yoshihara, Y. & Kuroda, K. O. Behavioral transition from attack to parenting in male mice: a crucial role of the vomeronasal system. *The Journal of neuroscience : the official journal of the Society for Neuroscience* **33**, 5120-5126, doi:10.1523/JNEUROSCI.2364-12.2013 (2013).

45   Vale, W., Spiess, J., Rivier, C. & Rivier, J. Characterization of a 41-residue ovine hypothalamic peptide that stimulates secretion of corticotropin and beta-endorphin. *Science* **213**, 1394-1397, doi:10.1126/science.6267699 (1981).

46   Ulrich-Lai, Y. M. & Herman, J. P. Neural regulation of endocrine and autonomic stress responses. *Nat Rev Neurosci* **10**, 397-409, doi:10.1038/nrn2647 (2009).

47   Betley, J. N., Cao, Z. F., Ritola, K. D. & Sternson, S. M. Parallel, redundant circuit organization for homeostatic control of feeding behavior. *Cell* **155**, 1337-1350, doi:10.1016/j.cell.2013.11.002 (2013).

48   Wang, L., Chen, I. Z. & Lin, D. Collateral pathways from the ventromedial hypothalamus mediate defensive behaviors. *Neuron* **85**, 1344-1358, doi:10.1016/j.neuron.2014.12.025 (2015).

49   Battagello, D. S. *et al.* Anatomical Organization of Urocortin 3-Synthesizing Neurons and Immunoreactive Terminals in the Central Nervous System of Non-Human Primates [Sapajus spp.]. *Front Neuroanat* **11**, 57, doi:10.3389/fnana.2017.00057 (2017).

50   Chen, P., Lin, D., Giesler, J. & Li, C. Identification of urocortin 3 afferent projection to the ventromedial nucleus of the hypothalamus in rat brain. *J Comp Neurol* **519**, 2023-2042, doi:10.1002/cne.22620 (2011).

51   Wittmann, G., Fuzesi, T., Liposits, Z., Lechan, R. M. & Fekete, C. Distribution and axonal projections of neurons coexpressing thyrotropin-releasing hormone and urocortin 3 in the rat brain. *J Comp Neurol* **517**, 825-840, doi:10.1002/cne.22180 (2009).

52   Yang, C. F. *et al.* Sexually dimorphic neurons in the ventromedial hypothalamus govern mating in both sexes and aggression in males. *Cell* **153**, 896-909, doi:10.1016/j.cell.2013.04.017 (2013).

53   Isogai, Y. *et al.* Molecular organization of vomeronasal chemoreception. *Nature* **478**, 241-245, doi:10.1038/nature10437 (2011).

54   Dobin, A. *et al.* STAR: ultrafast universal RNA-seq aligner. *Bioinformatics* **29**, 15-21, doi:10.1093/bioinformatics/bts635 (2013).

55   Mudge, J. M. & Harrow, J. Creating reference gene annotation for the mouse C57BL6/J genome assembly. *Mamm Genome* **26**, 366-378, doi:10.1007/s00335-015-9583-x (2015).

56   Turro, E. *et al.* Haplotype and isoform specific expression estimation using multi-mapping RNA-seq reads. *Genome Biol* **12**, R13, doi:10.1186/gb-2011-12-2-r13 (2011).

57   Turro, E., Astle, W. J. & Tavare, S. Flexible analysis of RNA-seq data using mixed effects models. *Bioinformatics* **30**, 180-188, doi:10.1093/bioinformatics/btt624 (2014).

58   Wagner, G. P., Kin, K. & Lynch, V. J. Measurement of mRNA abundance using RNA-seq data: RPKM measure is inconsistent among samples. *Theory Biosci* **131**, 281-285, doi:10.1007/s12064-012-0162-3 (2012).

44

59   Perez, J. D. *et al.* Quantitative and functional interrogation of parent-of-origin allelic expression biases in the brain. *Elife* **4**, e07860, doi:10.7554/eLife.07860 (2015).

45